NEt3-Triggered Synthesis of UHMWPE Using Chromium Complexes Bearing Non-innocent Iminopyridine Ligands

Lewis Base Additive−Triggered Synthesis of UHMWPE Using Non−Innocent Iminopyridine Chromium Complexes

Giorgia Zanchin,[a,τ] Alessandro Piovano,[b,τ] Alessia Amodio,[b] Fabio De Stefano,[c] Rocco Di Girolamo,[c,*] Elena Groppo,[b,*] Giuseppe Leone[a,*]

[τ] These authors contributed equally to the manuscript.

[a] CNR, Istituto di Scienze e Tecnologie Chimiche "Giulio Natta" (SCITEC), via A. Corti 12, I-20133 Milano, Italy.

[b] Dipartimento di Chimica, NIS Interdepartmental Research Center and INSTM Reference Center, Università degli Studi di Torino, Via G. Quarello 15A, I-10135 Torino, Italy.

[c] Dipartimento di Scienze Chimiche, Università di Napoli "Federico II", Complesso Monte S. Angelo, via Cintia, I-80126 Napoli, Italy.

*** Corresponding authors**

E-mail address: rocco.digirolamo@unina.it (R. Di Girolamo)

E-mail address: elena.groppo@unito.it (E. Groppo)

E-mail address: giuseppe.leone@scitec.cnr.it (G. Leone)

Abstract

Non-innocent iminopyridine chromium complexes were investigated as pre-catalysts for the polymerization of ethylene, using different aluminum co-catalysts and the Lewis base NEt_3 as additive. Beyond confirming the key role of the *chromium to ligand synergy* to access an active complex, other factors that play a crucial role are: (*i*) the nature of the aluminum activator that influences the cationic ion pair generated, (*ii*) the presence of the additive that boosts the synthesis of UHMWPE with narrow and unimodal molecular weight distribution even at 40 °C, and (*iii*) the polymerization temperature that affects the polymerization catalysis and the polymer molecular weight distribution. UV−vis−NIR and FT-IR spectroscopies have been applied to inspect the activation process and to understand the mode of action by which NEt_3 affects the catalytic conversion of ethylene. It is inferred that NEt_3 reacts with the aluminum co-catalyst (rather than with the chromium complex) to form an $Et_3N^*AlR_x$ adduct, thus affecting the catalytic ion pair.

KEYWORDS
polyethylene; UHMWPE; Chromium catalysis; UV-Vis-NIR spectroscopy; iminopyridines; additives; insertion polymerization.

1. INTRODUCTION

The polymerization of ethylene catalyzed by transition metal complexes is one of the most industrially relevant synthetic reactions and the development of high−performance catalysts continue to be a major driving force to access different polyethylene (PE) grades.[1–4] Beyond early and late transition metal catalysts,[5–7] chromium catalysts are also of great interest, both homogeneous,[8–10] and heterogeneous.[11–13] The peculiarity of homogeneous organochromium complexes is the ability to give from linear α-olefins (selective tri- and tetramerization) to high−density PE (HDPE), and even ultrahigh−molecular weight PE (UHMWPE). The selectivity may be obtained either by tuning the steric and electronic properties of the ligand,[8,9] or by using neutral donor molecules covalently linked to the organochromium complex.[14,15] Generally, chromium complexes are renowned for their ability in the oligomerization of ethylene,[16,17] while examples of chromium complexes for UHMWPE production are rare. These include chromium complexes bearing β−ketoimines and β−diketimines,[18] half−metallocene Cr(III) complexes bearing a N^O ligand,[19] and salicylaldiminate Cr(III) complexes.[20]

Alternative and effective strategies to tune the catalytic performance of homogeneous chromium complexes (*e.g.* in terms of reaction rate, productivity and molecular weight of the resultant PEs involve the usage of external additives (or modifiers).[21,22] For example, Rastogi *et al.* used 2,6-di-tert-butylphenol (BHT) to trap free−$AlMe_3$, present in commercially available methylaluminoxane (MAO) and responsible of fast chain-termination, to synthesize UHMWPE from a hemi−metallocene chromium catalyst.[21] Enders *et al*. demonstrated that the addition of a 9-borabicyclo[3.3.1]nonane enables the synthesis of UHMWPE from half−metallocene organochromium catalysts.[22]

The modifiers are usually small organic molecules having heteroatoms (N, O, and P) or metal salts (*e.g.*, $ZnCl_2$, $AlCl_3$, and BF_3), and they can be classified as Lewis acids or Lewis bases. Lewis acids are used to electronically depauperate the active site, favoring olefin coordination and insertion, and thereby increasing the rate of polymerization and productivity. Lewis base additives (*e.g.*, THF, ethyl benzoate, acetonitrile, PPh_3) coordinate to the most

acidic species over the course of the polymerization, namely the complex in its activated form and/or the Al−cocatalyst (*i.e.*, MAO or AlR_3). By steric shielding or electron density modification, the Lewis base additives modify the ratio between the rate constants of chain-propagation and chain-termination. Most of these modifiers have been previously reported to afford enhancements in the oligomerization and polymerization of ethylene catalyzed by zirconium,[23–25] cobalt,[26,27] vanadium,[28] tungsten,[29] and late transition metal based catalysts.[30–32] Despite the important beneficial effects in the use of additives to design competitive catalysts, the full potential of additives in selective polymerization of ethylene has not been investigated as well as their "activation" path remains elusive in many cases.

In this context, we recently reported the polymerization of ethylene catalyzed by simple and readily accessible iminopyridine chromium complexes in the formal oxidation state +2 (**Cr1**−**Cr3**) and +3 (**Cr4**) (Chart 1).[33] The chromium complexes differ in the nature of the substituents at the iminic carbon and at the *ortho*−aryl positions. We demonstrated that a concerted Cr−to−ligand electron transfer, coupled with a good stability of the $[(L^{\bullet})Cr^{III}]^{-}$ intermediate with the ligand in the monoanionic radical form $(L^{\bullet})^{-}$, is mandatory for providing an unexpected utility in the polymerization of ethylene. The obtained result was rather counterintuitive since iminopyridines were expected to give a poorly efficient shielding to stabilize the chromium active species, and thereby they were believed to have the right "structural" motif to generate catalysts for the oligomerization of ethylene but not for its polymerization.[34] Based on these results, herein, we expand our previous study to investigate and understand at a molecular level the effects of different aluminum activators, and of NEt_3 additive on the polymerization of ethylene mediated by **Cr1**. The new findings will be described as follows: at first, we will present the results of the catalytic tests, which confirm the key role of the *chromium to non-innocent iminopyridine synergy* and, more important, highlight that NEt_3 has a beneficial effect toward the synthesis of UHMWPE even at temperature as high as 40 °C. Then, we will discuss the results obtained by applying FT-IR and UV-Vis-NIR spectroscopies, which allow understanding the mode of action by which NEt_3 affects the catalytic conversion of ethylene.

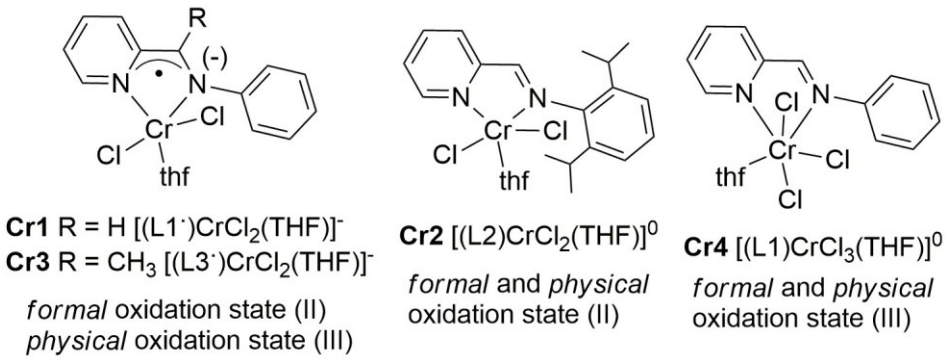

Chart 1. Iminopyridine chromium pre-catalysts **Cr1**−**Cr4**.

2. MATERIALS AND METHODS

2.1 General Procedures and Materials. Manipulations of air- and/or moisture-sensitive materials were carried out under an inert atmosphere using a dual vacuum/nitrogen line and standard Schlenk-line techniques with oven-dried glassware. Nitrogen and ethylene were purified by passage over columns of $CaCl_2$, molecular sieves, and BTS catalysts. Toluene (Aldrich >99.5%) was refluxed over Na for 8 h and then distilled and stored over molecular sieves. Dichloromethane (Aldrich, ≥99.8%) was dried by stirring over CaH_2 in inert atmosphere for 8 hours, distilled, and stored over 5Å molecular sieves away from bright light. Chloroform (Aldrich, ≥99%) was degassed with freeze-pump-thaw cycling and dried over Na_2SO_4. MAO (Aldrich, 10 %wt solution in toluene), diethylaluminum chloride (DEAC, Aldrich, 97%), triethylaluminum (TEAl, Aldrich, 93%), triisobutylaluminum (TIBA, Aldrich, 99%), diisobutylaluminum hydride (DIBALH, Aldrich, 99%), triethylamine (NEt_3, Aldrich, >99%), and deuterated solvent for NMR measurements ($C_2D_2Cl_4$) (Aldrich, >99.5% atom D) were used as received. TMA–depleted MAO (dMAO; TMA stands for $AlMe_3$) was prepared removing toluene and free $AlMe_3$ from commercially available MAO 10 %wt solution in toluene.

2.2 Synthesis of Chromium Complexes. All of the chromium complexes were synthesized following the method reported in our previous article.[33] **Cr1**–**Cr3** were synthesized by reaction of $CrCl_2$ with a stoichiometric amount of the corresponding ligand in THF at room temperature, while **Cr4** was prepared starting from $CrCl_3(THF)_3$.

2.3 Polymerization Procedures. Polymerization of ethylene was carried out in a 50 mL round-bottomed Schlenk flask. Prior to the start of polymerization, the reactor was heated to 110 °C under vacuum for 1 h and backfilled with nitrogen. For ethylene polymerization, the reactor was charged at room temperature with toluene and the cocatalyst in that order. After thermal

equilibration at the desired temperature, the solution was degassed, and ethylene was added until saturation. When a precontact between the additive and the complex was required, the two components were premixed in a 25 mL Schlenk for 1 minute. Polymerization was started by adding a dichlorometane solution (2 mg mL^{-1}) of the chromium complex via syringe under a continuous flow of ethylene. Polymerizations were stopped with methanol containing a small amount of hydrochloric acid; the precipitated polymers were collected by filtration, repeatedly washed with fresh methanol, and finally dried under vacuum at room temperature to constant weight.

In all of the reactions investigated, no polymerization activity was observed in the absence of the chromium source.

2.4 Characterization Methods.

2.4.1. Polymer Characterization

Molecular weight (M_w) and molecular weight distribution (M_w/M_n) were obtained by a high-temperature Waters GPCV2000 size exclusion chromatography (SEC) system using an online refractometer detector. The experimental conditions consisted of three PL Gel Olexis columns, *o*-dichlorobenzene as the mobile phase, 0.8 mL min^{-1} flow rate, and 145 °C temperature. The calibration of the SEC system was constructed using 18 narrow M_w/M_n PS standards with M_w values ranging from 162 to 5.6×10^6 g mol^{-1}. For SEC analysis, about 12 mg of polymer was dissolved in 5 mL of *o*-dichlorobenzene. The calorimetric measurements were performed with a Mettler-DSC822 operating in N_2 atmosphere. The sample, typically 5 mg, was placed in a sealed aluminum pan, and the measurement was carried out from −70 to 180 °C using a heating and cooling rate of 10 °C min^{-1}. T_m and ΔH_m values were recorded during the second heating. The X-ray powder diffraction profiles of the as-prepared samples were obtained with Ni filtered Cu Kα radiation (wavelength λ=0.15418 nm) by using an Empyrean diffractometer by Panalytical operating in the reflection geometry. FT-IR spectra were acquired using a Perkin–Elmer Spectrum Two in attenuated total reflectance mode in the spectral range of 4000–500 cm^{-1}.

2.4.2. *Characterization of the pre-catalysts and catalysts*

FT-IR and UV-Vis-NIR spectra of the organometallic compounds were measured in transmission mode, by dissolving the complexes in chloroform (10^{-3} mol L^{-1}), adding when necessary the Al-alkylators and the NEt_3 additive in stoichiometric amount (Al/Cr = 10 and N/Cr = 20, respectively). FT-IR spectra were collected in the spectral range of 7000−400 cm^{-1},

containing the solution in a Specac Omni cell with KBr windows, and using a Bruker Alpha spectrophotometer that was placed inside the glovebox to avoid sample contamination. UV−Vis−NIR absorption spectra were collected using a Cary5000 spectrophotometer, the solutions were measured inside homemade cells equipped with windows in optical quartz (Suprasil), filled inside the glovebox and closed with Teflon plugs. For both techniques, the spectrum of the solvent was measured under the same conditions and subtracted from those of the samples.

3. RESULTS and DISCUSSION

3.1 Catalytic screening

3.1.1 *The selection of the Al−activator*

A baseline catalytic behavior of **Cr1** activated with various aluminoxanes and aluminum alkyls was first established. The selected Al−activators were MAO, dMAO, DEAC, TIBA and DIBALH. The polymerizations were performed in toluene at an ethylene pressure of 1 atm, room temperature, and 250 equiv. of Al to Cr. Low chromium catalyst loading and short reaction time were employed to easily keep constant the temperature throughout the polymerization without cooling in the early stages, to maintain homogeneous physical conditions and to avoid side reactions caused by gel effect and high mixture viscosities.

The use of different Al−cocatalysts had a considerable effect on the catalytic behavior. The only productive run was obtained with MAO (Table S1), whereas dMAO and all the aluminum alkyls entirely stop the catalysis, resulting in a loss of activity for **Cr1**. We hypothesized that the positive effect of MAO relies on its ability of generating large counterions around the active species (sharply simplified with the formula $L_nMtMe^+ \cdots ClMAO^-$), less coordinating than the R_3AlCl^- anions, generated with the other Al−cocatalysts.[35–37] It can be inferred that the formation of a looser ion pair, as the one formed with **Cr1**/MAO, is fundamental to exhibit ethylene polymerization activity. Conversely, the formation of a tight ion pair in the presence of DEAC, TIBA, and DIBALH may inhibit subsequent insertions of ethylene or somehow facilitates a faster chain-termination over chain-propagation. This is in line with earlier results reported by Nomura and Zhang, who described a high tendency for β−hydride elimination and subsequent chain-termination for vanadium complexes with aluminum alkyls.[38] Alternatively, modification of the **Cr1** ligand skeleton may also be an alternative scenario to explain the lack of activity of **Cr1**/AlR_3. For instance, a

reduction of the iminic C=N bond in phenoxyimine Group 4 complexes by DIBALH and TIBA is documented.[39,40]

Meanwhile, we were puzzled by the inactivity of **Cr1** when dMAO was employed as cocatalyst, since it is well established and documented that oligomeric $(AlOMe)_n$ cages possess intrinsic alkylating capabilities and likely play a prominent role over TMA.[41,42] In such an event, we therefore speculate that the presence of free−TMA in commercial MAO solution is somehow essential for polymerization activity. Given the monoanionic radical $(L^{\bullet})^{-}$ state of the ligand in **Cr1** (Chart 1) and the high sensitivity of chromium, it can be inferred that the TMA plays a fundamental role by acting as oxygen and impurities scavenger that otherwise would poison the catalytic system.

3.1.2 *The effect of Lewis base NEt_3 additive on the catalytic performance*

Subsequently, we investigated the effect of the addition of NEt_3 on the catalytic behavior of **Cr1**/MAO. A solution of **Cr1** was treated with NEt_3 prior to activation with MAO and ethylene injection. A first screening was performed at room temperature, at atmospheric ethylene pressure and by varying the NEt_3 concentration while the Cr-complex concentration was maintained constant. Polymerization conditions and results are summarized in Table 1. **Cr2**–**Cr4** (Chart 1) were also investigated for comparison.

Table 1. Polymerization of ethylene by **Cr1**−**Cr4**/MAO and with the addition of NEt_3.[a]

entry	Cr	NEt_3 (μmol)	NEt_3 (equiv. to Cr)	yield (mg)	activity[b]	M_w[c] (g mol^{-1})	M_w/M_n[c]	T_m[d] (°C)	ΔH_m[d] (J g^{-1})
1	**Cr1**			183	2290	1.0×10^5	4.8	131.9	252
2	**Cr1**	2.5	1	156	2076	2.3×10^5	6.9	137.0	205
3	**Cr1**	12.5	5	186	2475	2.9×10^5	7.1	139.2	184
4	**Cr1**	25	10	192	2400	4.5×10^5	10.4	134.4	230
5	**Cr1**	37.5	15	234	2925	1.2×10^6	7.5	137.0	204
6	**Cr1**	50	20	235	2940	$> 2\times10^6$	5.3	137.6	159
7	**Cr1**	125	50	115	1440	$> 2\times10^6$	6.1	139.7	167
8	**Cr2**	50	20	−					
9	**Cr3**	50	20	−					
10	**Cr4**	50	20	−					

[a] polymerization conditions: ethylene pressure, 1.01 bar; total volume, 25 mL (toluene); Cr complex, 2.4 μmol, complex solution in dry dichloromethane; Al/Cr = 250, Al = MAO; time, 2 min; temperature, 20 °C. [b] activity in $kg_{pol}\ mol_{Cr}^{-1}\ h^{-1}$; [c] determined by SEC; [d] determined by DSC. NEt_3 was stirred with the solution of pre-catalyst for 1 min before they were charged in the reaction flask.

The data in Table 1 reveal that the addition of NEt_3 leads to significant changes in the catalysis employing **Cr1**. As a matter of fact, the catalytic activities for **Cr1**, in the presence of

the basic additive, are all very high and for 15 and 20 equiv. of NEt_3 added even higher than in the absence of the additive. The test with a large excess of the additive (50 equiv. to Cr, entry 7) is an exception. At N/Cr = 50 the activity strongly decreases, suggesting that a higher concentration of NEt_3 may interfere with the ethylene coordination/insertion and/or in any case poison the chromium pre-catalyst, resulting in a significant reduction in activity.

An even more interesting result is the molecular weight of the obtained polymers. The addition of NEt_3 leads to an increase of the PE molecular weight, while keeping the molecular weight distribution rather narrow and unimodal ($5.3 < M_w/M_n < 10.4$). Addition of 1 equiv. of NEt_3 led to a doubling in molecular weight, while addition of 10 equiv. of NEt_3 gave rise to a four-fold increase of the molecular weight. The increase in the polymer molecular weight is especially significant when 20 or more equivalents of NEt_3 were employed: in those cases, the obtained polymers are UHMWPEs, where the number-average molar mass determined by GPC exceeds 2×10^6 g mol^{-1} and even up to 5×10^6 g mol^{-1} that cannot be conclusively ascertained with the size exclusion chromatography technique. Indeed, for polymers having molar mass above 10^6 g mol^{-1} the application of the existing chromatography technique becomes challenging to provide the desired information.[43] Melt rheometry may be successfully utilized to measure the molar mass and polydispersity of the obtained UHMWPEs, but such analysis is beyond the scope of this article. Nonetheless, the obtained findings are of high relevance because they show that it is possible to tune the PE molecular weight over a broad range by using **Cr1** and different amounts of NEt_3, without changing the reaction conditions and/or the ligand set.

Overall, the addition of the NEt_3 has a positive influence on both the catalytic activity and on the polymer molecular weight. This effect is correlated to the amount of NEt_3 added, the optimal conditions identified being at NEt_3/**Cr1** = 20. It is likely to expect that when 20 equiv. of the amine are added, all the active species are homogeneously influenced, as indicated also by the narrower molecular weight distribution at increasing NEt_3/**Cr1** ratio. A further increase to NEt_3/**Cr1** = 50 is detrimental. This might be due to: (*i*) a sort of drowning of the catalytically active species by the additive, resulting in inhibition of monomer coordination, and (*ii*) a possible "degradation" of MAO through adduct formation which disrupts dative Al···O bonding. This last scenario has been documented for pyridine and bipyridine,[44] hence it is plausible that NEt_3 behaves analogously.

The molecular weight strongly affects the thermal properties of the obtained PEs. DSC second heating scans reported in Figure 1 indicate that all samples present a single melting temperature (T_m) with a melting peak that increases with increasing molecular weight.[45] In particular, the melting temperature ranges from 131.9 °C (entry 1 in the absence of the additive) to 139.7°C (entry 7 at NEt_3/Cr = 50).

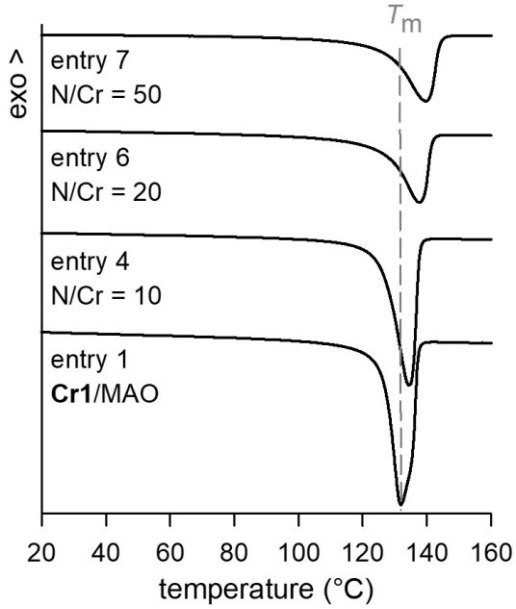

Figure 1. DSC second heating scans recorded at 10 °C min^{-1} of entries **1** (in the absence of NEt_3) and **4**, **6** and **7**.

Finally, **Cr2**–**Cr4**, not active in the absence of the additive,[33] show no activity even in the presence of NEt_3 (Table 1, entries 8–10). It is therefore reasonable to assume that the additive has no effect on the "activation" path of **Cr2**–**Cr4** and to ascertain definitively that the nature of the iminopyridine substituents plays a fundamental role in the catalytic transformation of ethylene regardless of the presence of the additive: necessary conditions for ethylene polymerization are the Cr–to–ligand synergy (*i.e.*, the tendency of chromium to undergo one-electron transfer to the ligand) and the good stability of the active intermediate in the presence of the Al−activator, both conditions fulfilled only by **Cr1**.[33]

3.1.3 *Polymerization of Ethylene by Cr1/MAO/NEt_3 at different temperature*

A series of polymerization were performed at different temperature with a feed of 250 equiv. of MAO and 20 equiv. of NEt_3. The same tests in the absence of NEt_3 were performed for comparison. Polymerization conditions and results are summarized in Table 2.

Generally, when the temperature was enhanced, a smooth decrease in the activity was observed, both without and with the additive. While a decrease in ethylene solubility at elevated

temperatures may play a key role, the major effect of the temperature on the activity should be attributed to an increased instability of the Cr−alkyl bond in the active species and subsequent catalyst decay, which both correlate with a dominant chain-transfer.[46]

Table 2. Polymerization of ethylene catalyzed by **Cr1**/MAO and with the addition of NEt_3.[a]

entry	NEt_3 (equiv. to Cr)	T (°C)	yield (mg)	activity[b]	M_w[c] (g mol^{-1})	M_w/M_n[c]	T_m[d] (°C)	ΔH_m[d] (J g^{-1})
1		20	183	2288	1.0×10^5	4.8	131.9	252
11		40	160	2000	7.7×10^4	13.0	130.8	223
12		60	167	2090	1.2×10^5	17.4	130.1	219
6	20	20	235	2940	$> 2\times10^6$	5.3	137.6	159
13	20	40	192	2400	1.4×10^6	1.6	137.9	165
14	20	60	189	2360	6.6×10^4	4.4	131.6	250

[a] polymerization conditions: ethylene pressure, 1.01 bar; total volume, 25 mL (toluene); Cr complex, 2.4 μmol, complex solution in dry dichloromethane; Al/Cr = 250, Al = MAO; time, 2 min. [b] activity in kg_{pol} mol_{Cr}^{-1} h^{-1}; [c] determined by SEC; [d] determined by DSC. In entries 6, 13 and 14, NEt_3 (50 μmol) was stirred with the solution of pre-catalyst for 1 min before they were charged in the reaction flask.

All the obtained PEs are fully saturated, semicrystalline polymers. The formation of saturated PEs can be accounted for by a chain-termination path involving chain-transfer to the aluminum. In the absence of the additive, the properties of the resultant PEs resemble those of PEs by heterogeneous chromium−silica catalysts with M_w/M_n in the range 4.8−17.4 (M_w of about 1.0×10^5 g mol^{-1}). Increasing the reaction temperature, the chain-transfer becomes predominant, the shape of the SEC curves strongly depending on the polymerization temperature (Figure 2a-c, black curves). Particularly at 60 °C the SEC curve is dominated by two components with a low-MW and a high-MW fraction centered at 7000 and 1×10^5 g mol^{-1}, respectively (Figure 2a, black curve). This uniquely indicates the presence of several active species under certain polymerization conditions. On the opposite, the catalytic system **Cr1**/MAO/NEt_3 matches a good performance in terms of selectivity toward nearly monodisperse UHMWPE even at 40 °C (Figure 2b, green curve). Indeed, a net effect of the additive is that **Cr1**/MAO/NEt_3 produces more polymer chains of comparable molecular weight ($1.6 < M_w/M_n < 5.3$) than **Cr1**/MAO.

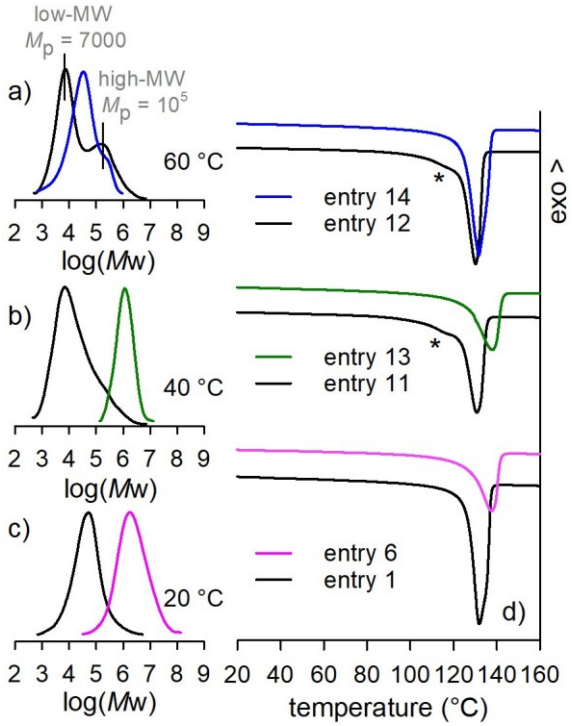

Figure 2. (a) SEC traces (refractive index plots) of PEs obtained by **Cr1**/MAO (black) and **Cr1**/MAO/NEt_3 (blue) at 60°C (M_p is the peak molecular weight as g mol^{-1}); (b) SEC traces (refractive index plots) of PEs obtained by **Cr1**/MAO (black) and **Cr1**/MAO/NEt_3 (green) at 40°C; (c) SEC traces (refractive index plots) of PEs obtained by **Cr1**/MAO (black) and **Cr1**/MAO/NEt_3 (pink) at 20°C; (d) DSC second heating scans recorded at 10 °C min^{-1} of PEs obtained by **Cr1**/MAO (black) and PEs obtained by **Cr1**/MAO/NEt_3 (colored lines).

Differences in polydispersity and/or molecular weight of the obtained PEs are reflected in their thermal properties. The DSC heating curves of the PEs crystallized from the melt are reported in Figure 2d (T_m and ΔH_m in Table 2). DSC experiments confirm the previously observed relationship between molecular weight and melting temperature. In addition, it is worth noting that sample **11** and **12**, synthesized in the absence of the additive and at 40 and 60 °C, respectively, and presenting broad molecular weight distribution ($13 < M_w/M_n < 17$) and a bimodal character, show a shoulder in the DSC endotherms at temperatures lower than that of the main peak (marked with an asterisk). This may be likely due to the melting of PE crystals originated from low-MW PE fractions, which, on the other hand, are not formed in the presence of the additive. WAXS patterns performed on samples of Table 1 and Table 2 show the presence of PE crystals in the orthorhombic form with a small amount of monoclinic form (Figure S1).

~~To sum up the experimental results presented so far, we observed that the presence of NEt_3 has a remarkable and beneficial effect, mitigating chain transfer and favoring the growth~~

~~of the macromolecular chain over the side reactions that bring to chain "release". The action mode of the additive will be the object of investigation in the following paragraphs.~~

3.2 What is the role of NEt_3? A spectroscopic study

To sum up the experimental results presented so far, the presence of NEt_3 has a remarkable and beneficial effect on the polymerization of ethylene by **Cr1** in the presence of Al-cocatalysts, mitigating the chain-transfer and favoring the growth of the macromolecular chain over the side reactions that bring to chain "release". To formulate some mechanistic hypothesis, however, it is necessary to understand how NEt_3 interacts with all the components in the system. Considering that NEt_3 is a Lewis base, it can potentially interact with all the inorganic and organometallic compounds in the system that have a Lewis acidic character, namely the Al−cocatalyst, the chromium complex, and the cationic active species generated by the interaction of **Cr1** with the aluminum cocatalyst. All these interactions are expected to be weak coulomb interactions rather than covalent bonding, but which interaction(s) actually take place is not known a priori. In order to answer to this question, we performed a series of experiments by UV-Vis-NIR and FT-IR spectroscopies, whose use in the field of Cr-based catalysts for olefin polymerization is well assessed.[Groppo et al. Chem. Rev. 2005, 105, 115-183; Catal. Sci. Technol., 2013, 3, 858; Groppo et al. ACS Catal. 2018, 8, 10846−10863]

Figure 3a shows the UV-Vis-NIR spectra of the **Cr1** complex and of the **Cr1**/NEt_3/MAO system. The spectrum of **Cr1** is characterized by well-defined bands at 30200, 20000, 16500, 14000, 10500 and 5500 cm^{-1}, that were previously assigned to the π-π* transitions of the ligand in the π-radical monoanionic $(L^{\bullet})^{-}$ form (being the spectrum of the neutral ligand L characterized only by bands above 24000 cm^{-1}).[33] After the contact with NEt_3 and MAO, the band at 30200 cm^{-1} decreases in intensity and slightly downward shifts, while all the others disappear. The same behavior was observed upon contacting **Cr1** with NEt_3 and TEAl, as shown in Figure 3b. In both cases, a much weaker band seems to appear at ~23000 cm^{-1}, more evident for TEAl than for MAO. These results indicate that after the contact with NEt_3 and the aluminum activator, the electronic properties of **Cr1** dramatically change. In particular, the disappearance of the bands diagnostic for the $(L^{\bullet})^{-}$ ligand univocally indicates that the ligand goes back to its neutral (L) form. This is independent from the type of aluminum activator, corroborating the hypothesis that all the aluminum cocatalysts generate chromium active sites with the same electronic properties, even though only MAO activates **Cr1** for

ethylene polymerization. For this reason, we decided to perform the spectroscopic study by using TEAl as cocatalyst, since its spectroscopic features are much simpler than those of MAO.

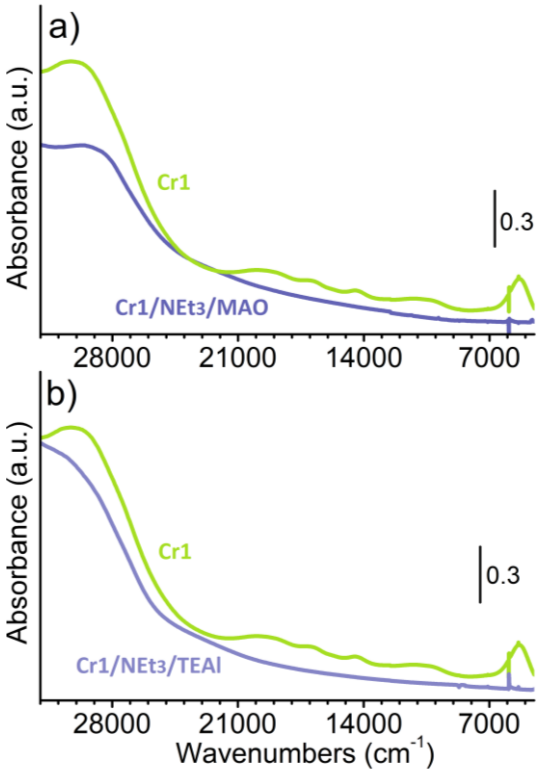

Figure 3. UV-Vis-NIR spectra of **Cr1** and **Cr1**/NEt_3/MAO (part a) and **Cr1**/NEt_3/TEAl (part b) (Cr = 10^{-3} M in $CHCl_3$, Al/Cr = 10, N/Cr = 20).

The interpretation of the UV-Vis spectra of the ternary **Cr1**/NEt_3/TEAl system (and even more of the IR spectra) is not straightforward, and requires to know not only which are the spectroscopic fingerprints of each component alone, but also which are the spectroscopic manifestation of all the possible binary systems, namely **Cr1**/NEt_3, **Cr1**/TEAl and NEt_3/TEAl.

3.2.1 Cr1/NEt_3

Figure 4 shows the UV-Vis-NIR and FT-IR spectra of **Cr1**, NEt_3 and their mixture. The UV-Vis spectrum of **Cr1** was already commented above, that of NEt_3 does not show any absorption band in the investigated spectral range, and that of **Cr1**/NEt_3 is almost the same as that of **Cr1**. The FT-IR spectrum of **Cr1**/NEt_3 is the bare sum of those of **Cr1** and NEt_3. Both evidences univocally indicate that NEt_3 does not interact with **Cr1**, even though there are a few cases in the literature reporting interactions between metallocene pre-catalysts and Lewis bases.[24,25,47]

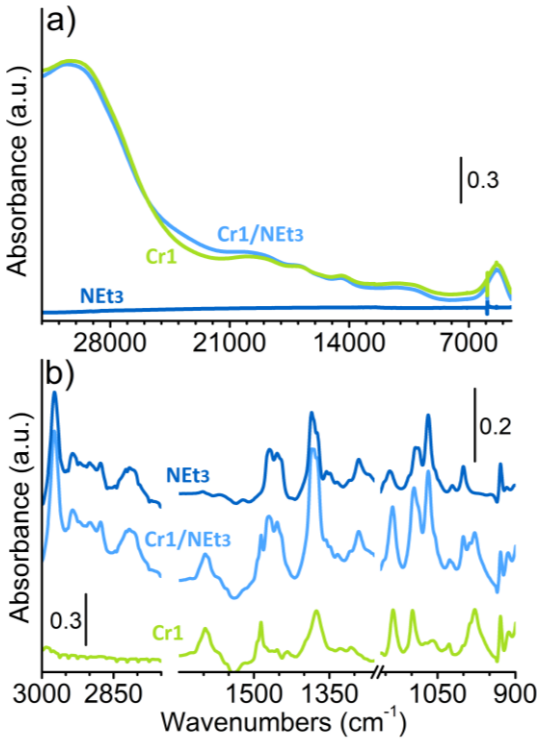

Figure 4. UV-Vis-NIR (part a) and FT-IR (part b) spectra of **Cr1**, NEt_3 and **Cr1**/NEt_3 in chloroform (Cr = 10^{-3} M in $CHCl_3$, N/Cr = 20).

3.2.2 Cr1/TEAl

A different spectral behavior is observed when contacting **Cr1** with TEAl, as reported in Figure 5. The UV-Vis-NIR spectrum of **Cr1**/TEAl (Figure 5a) is very similar to that of the **Cr1**/TEAl/NEt_3 discussed above (Figure 3b). Upon interaction of **Cr1** with TEAl, the absorption bands due to the π–π* transitions of the ligand in its $(L^{\bullet})^-$ radical form disappear, indicating that, upon **Cr1** activation, the ligand goes back to its neutral L form.[33]

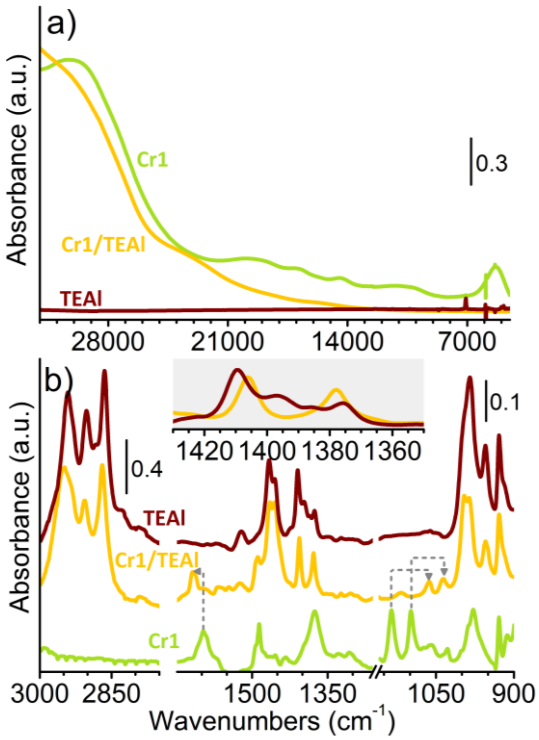

Figure 5. UV-Vis-NIR (part a) and FT-IR (part b) spectra of **Cr1**, TEAl and **Cr1**/TEAl (Cr = 10^{-3} M in $CHCl_3$, Al/Cr = 10). The inset in part b) shows a magnification of the 1430 – 1360 cm^{-1} region, which contains the absorption bands due to the $\delta(CH_2)$ and $\delta_{sym}(CH_3)$ vibrational modes. The dashed arrows indicate the shifts of the bands of **Cr1** after interaction with TEAl.

FT-IR spectroscopy (Figure 5b) confirms that **Cr1** and TEAl interact together. The IR spectrum of **Cr1** shows a series of absorption bands in the 1700−900 cm^{-1} region, which are due to the vibrations of the $(L^{\bullet})^{-}$ radical anionic ligand. These bands are still visible in the spectrum of **Cr1**/TEAl, but shifted in different positions and much less intense, as expected if $(L^{\bullet})^{-}$ is transformed into neutral L. Indeed, the absorption bands due to the vibrations of the radical anion of a conjugated molecule are strongly enhanced in intensity in comparison to the corresponding neutral form. For example, the band at 1597 cm^{-1} in the spectrum of **Cr1** is observed at 1618 cm^{-1} in the spectrum of **Cr1**/TEAl, while the doublet at 1135−1098 cm^{-1} shifts at 1062−1035 cm^{-1}. As far as the spectrum of TEAl is concerned, characteristic bands are observed in the ranges 3000−2800 cm^{-1} (CH_x stretching modes), 1500−1300 cm^{-1} (CH_x bending modes) and 1000−900 cm^{-1} (C-C stretching modes). All these bands are observed in the spectrum of **Cr1**/TEAl but shifted. The most informative region is the 1430–1360 cm^{-1} one, which contains the absorption bands due to the $\delta(CH_2)$ and $\delta_{sym}(CH_3)$ vibrational modes. The spectrum of TEAl shows four bands at 1410, 1397, 1385 and 1375 cm^{-1}, which are specific for

TEAl in the dimeric form.[48] This explains why both the $\delta(CH_2)$ and $\delta_{sym}(CH_3)$ vibrational modes are split in two bands: the ethyl groups bridging the two Al cations behave differently from the others, and are responsible for the two bands at 1397 cm^{-1}, $\delta(CH_2)$, and 1385 cm^{-1}, $\delta_{sym}(CH_3)$. The spectrum of **Cr1**/TEAl is much simpler in this region, where only two bands are observed at 1406 and 1377 cm^{-1}, which are attributed to the $\delta(CH_2)$ and $\delta_{sym}(CH_3)$ vibrational modes of TEAl in its monomeric form. This observation indicates that most of the TEAl dimers are dissociated upon reaction with **Cr1**.

All in all, UV-Vis-NIR and FT-IR spectroscopies allow us to formulate a mechanistic hypothesis for the interaction between **Cr1** and dimeric TEAl, as sketched in Scheme 1: 1) a Cl^- ligand is substituted by an alkyl group, with the consequent release of AlR_2Cl; 2) a second Cl^- ligand is removed by coordinated AlR_3 with the subsequent creation of the coordination vacancy and the generation of an ion-pair between the cationic chromium complex and the anionic Al-alkyl moiety; 3) a further electronic rearrangement occurs, whereby the unpaired electron of the $(L^{\bullet})^-$ ligand drains onto the chromium ion, leading to a cationic Cr(II) complex, which has all the elements to be potentially active in ethylene polymerization, *i.e.* an alkyl ligand, a coordination vacancy and an effective positive charge, in agreement with the mostly accepted theory for homogeneous polymerization catalysis.

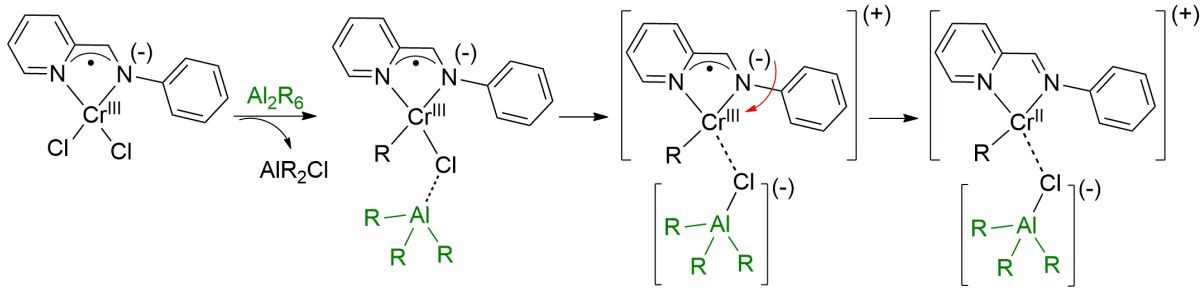

Scheme 1. Mechanistic hypothesis for the interaction between **Cr1** and TEAl, as derived from the spectroscopic data.

3.2.3 NEt_3/TEAl

The interaction between aluminum compounds and amines is well accepted in the literature. In the field of olefin polymerization, the complexation of free−TMA in commercial MAO solution with aromatic amines (namely pyridine and bipyridine) is one of the possible strategies for determining its amount.[44,49,50] Spectroscopy may help in understanding the kind of interaction. In this case, UV-Vis-NIR spectroscopy is not useful, since both TEAl and NEt_3 have no absorptions in the investigated region. In contrast, FT-IR spectroscopy does help.

Figure 6 shows the FT-IR spectra of NEt_3/TEAl and of the two compounds alone. The spectrum of NEt_3 shows absorption bands in three main ranges: in the 3000−2800 cm^{-1} ($\nu(CH_x)$ modes), in the 1500−1300 cm^{-1} ($\delta(CH_2)$ and $\delta(CH_3)$), and in the 1100-1000 cm^{-1} (ν(C-N) and ν(C-C)). In particular, the band of ν(C-N) at 1067 cm^{-1} is the most sensitive to the interaction of NEt_3 with Lewis acids. In the spectrum of NEt_3/TEAl this band shifts down to 1046 cm^{-1}, indicating that the two compounds combine together. An analogous shift was observed for the interaction between the tertiary amine NMe_3 in adduct with the Lewis acid BH_3.[51] Even more informative is the 1430−1360 cm^{-1} region, which is highlighted in the inset of Figure 6. The spectrum of NEt_3 shows only two bands at 1385 and 1374 cm^{-1}, which are assigned to $\delta(CH_2)$ and $\delta(CH_3)$ modes, opposite to the case of TEAl where four bands are observed due to its dimeric form (*vide supra*). Interestingly, the spectrum of NEt_3/TEAl is characterized by two very intense bands at 1395 and 1385 cm^{-1}, which are specific for the bending modes of bridging ethyl groups. These bands are remarkably more intense than in the spectrum of TEAl and indicate that a strong interaction is taking place between NEt_3 and TEAl. This is in agreement with the literature reporting that many Lewis bases (B) reversibly interact with aluminum alkyls,[52] cleaving the alkyl-bridged dimers to form new adducts, according to the equation $Al_2R_6 + 2B \rightleftharpoons 2(B{*}AlR_3)$.[49] The number of bridging ethyl groups increases from the two of TEAl dimer (left side of equation) to four (two groups per two NEt_3*TEAl adducts, right side of equation), as detailed in Scheme S1. Hence the total amount of bridging ethyl groups roughly doubles.

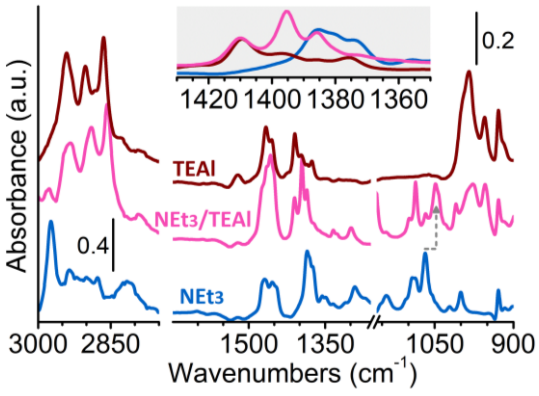

Figure 6. FT-IR spectra of NEt_3, TEAl and NEt_3/TEAl (in $CHCl_3$). The inset shows a magnification of the 1430 – 1360 cm^{-1} region, which contains the absorption bands due to the $\delta(CH_2)$ and $\delta_{sym}(CH_3)$ vibrational modes. The dashed arrow indicates the shift of the ν(C-N) band of NEt_3 after interaction with TEAl.

3.2.4 Cr1/NEt$_3$/TEAl

When all the three actors are mixed, the situation is more complex and requires the complementarity of the characterization techniques to get a unified picture. From the electronic point of view (Figure 7a), the effect of the activation of **Cr1**/NEt$_3$ by TEAl on the UV–Vis spectrum is analogous to that observed upon the activation of **Cr1** alone. The spectroscopic manifestations of the ligand in its radical anionic form disappear. FT–IR spectroscopy indicates the presence of NEt$_3$*TEAl adducts, as revealed by the ν(C-N) band at 1046 cm^{-1} and the two intense bands at 1395 and 1385 cm^{-1} due to the $\delta(CH_2)$ and $\delta(CH_3)$ modes of bridging ethyl groups.

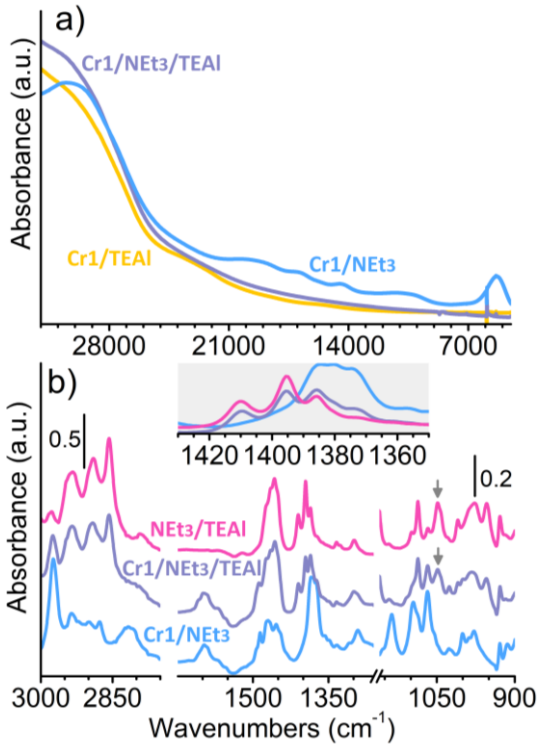

Figure 7. Part a): UV-Vis-NIR spectra of **Cr1**/NEt$_3$, **Cr1**/TEAl, and **Cr1**/NEt$_3$/TEAl (Cr = 10^{-3} M in $CHCl_3$, Al/Cr = 10, N/Cr = 20). Part b) FT-IR spectra of **Cr1**/NEt$_3$, NEt$_3$/TEAl and **Cr1**/NEt$_3$/TEAl (Cr = 10^{-3} mol L^{-1} in $CHCl_3$, Al/Cr = 10, N/Cr = 20). The inset in part b) shows a magnification of the 1430–1360 cm^{-1} region, which contains the absorption bands due to the $\delta(CH_2)$ and $\delta_{sym}(CH_3)$ vibrational modes. Grey arrows indicate the ν(C-N) band of NEt$_3$ in interaction with TEAl.

Therefore, all together these data suggest that, among all the possible equilibria of NEt$_3$ in the reaction mixture (as described in the previous paragraph), the only one that is actually photographed by UV–Vis–NIR and FT–IR spectroscopy is that involving the Al–activator, and this is likely the reason behind the great influence of NEt$_3$ on the ethylene polymerization

catalysis. In Scheme 2 a sketched hypothesis for the active chromium site is depicted as emerging from the spectroscopic analysis.

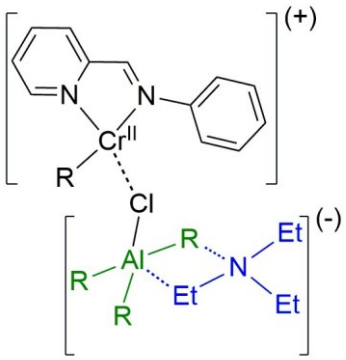

Scheme 2. Active species resulting from the activation of **Cr1** by AlR_3 in the presence of NEt_3.

3.3 NEt_3 and its role behind the scenes

The spectroscopic data discussed so far suggest that the nature of the active chromium species does not change significantly in terms of oxidation state and coordination environment whether it has been activated by TEAl or by MAO (both alone, as reported in our previous work,[33] and in the presence of NEt_3, as shown in Figure 3). Hence the different behavior of the two catalysts, namely **Cr1**/TEAl and **Cr1**/MAO (as discussed in paragraph 3.1.1), can be ascribed to the different influences of the respective counterions on the olefin coordination/insertion path.[35–37] Moreover, MAO and TEAl behave in the same manner with respect to the presence or absence of NEt_3, confirming the general relevance of the spectroscopic insights achieved on the **Cr1**/TEAl/NEt_3 system.

Therefore, even if the structural complexity of MAO and its variable content of free TMA prevent drawing of an univocal picture for the NEt_3 influence on the catalytic process (we cannot even incontrovertibly discriminate between NEt_3 interacting with either $[AlOMe]_n$, structural−TMA or free−TMA), contrarily to what has been obtained for the TEAl−activated **Cr1**/NEt_3 catalyst, some hypotheses can be sketched and are presented hereafter.

The first possibility is that NEt_3 coordinates only with free−TMA: as reported above, aromatic amines can be used to trap it, analogously to what BHT does.[44,53] This would explain the increase in the molecular weight of the resulting PE, since the chain-transfer to the Al−compound is one of the main chain-termination path (molecular weight decreased increasing the Al/Cr ratio).[33] An analogous increase in the molecular weight of PE by trapping the free−TMA with different molecules (namely, BHT and 9-BBN) is documented.[21,22] Moreover, TMA can form heterodinuclear adducts with the metal complexes interposing in the

ionic pair (as L_n**Mt**$(Me)_2Al(Me)_2^+ \cdots ClMAO^-$), a situation that is considered as dormant species toward olefin polymerization and connected with several decomposition or chain-termination pathways.[54] In this regard, trapping the free−TMA would explain also the increase in the overall catalytic activity.

The second possibility is that NEt_3 interacts with the other Al species of the cocatalyst, namely oligomeric MAO or the structural−TMA present, helping the stabilization of the negative charge by delocalization once the active species is formed. Whether NEt_3 interacts with structural−TMA or with MAO itself, the effect would be the same of increasing the steric hindrance of the anion and helping the charge dissipation in the ion pair. Both these modifications bring to the generation of weakly or less coordinating anions, which allow for an easier "approach" of the incoming monomer to the active site, facilitating its polymerization.[36,37,55,56] The importance of having a large anion (and hence a looser ion pair) for **Cr1** to be active in the polymerization of ethylene has been already proved by the fact that all the other Al−alkyls, that generate a tighter ion pair, are ineffective and stop the catalysis (Table S1).

At this point is hard to state which one of the two hypotheses takes place, and it might also be that both situations coexist at the same time. Additional insights are expected in the future by investigating the action mode of different Lewis base additives.

CONCLUSIONS

Herein we investigate the catalytic conversion of ethylene mediated by the iminopyridine **Cr1** complex in the presence of a series of Al−activators and with the addition of NEt_3. The results demonstrate that the choice of the proper aluminum alkyl is crucial for the complex to be active, and that the addition of NEt_3 in variable amounts allows the formation of PE with modular molecular weight, from high to ultra-high, and narrow and unimodal M_w/M_n even at temperature as high as 40 °C. This is rather unusual for molecular chromium complexes that are generally intended for ethylene oligo-, tri- or tetramerization. To define the precise mechanism of action of the amine additive we have performed a systematic FT-IR and UV–Vis–NIR spectroscopic study. The spectroscopic data demonstrate the occurrence of an interaction between NEt_3 and the Lewis acidic Al−activator, which brings to the formation of a looser ion pair and, consequently, is beneficial to boost the synthesis of UHMWPE.

In conclusion, this work demonstrates how the thoughtful introduction in the catalytic process of a simple and cheap additive as NEt_3 may largely improve the value-chain of the resulting product. UHMWPE is an engineering and smart polymer: it has high wear-resistance, toughness, durability, and biocompatibility that make it useful in many fields such as chemical, machinery, joint replacements, and other fields.

DECLARATION OF COMPETING INTEREST

The authors declare that they have no known competing financial interests or personal relationships that could have appeared to influence the work reported in this paper.

ACKNOWLEDGEMENTS

Funding: This work was supported by the project "Cr4FUN − Chromium catalysis: from fundamental understanding to functional aliphatic polymers" funded by MIUR *Progetti di Ricerca di Rilevante Interesse Nazionale (PRIN) Bando 2017* (20179FKR77_002).

SUPPORTING INFORMATION

Polymerization of ethylene by **Cr1** in combination with different aluminum co-catalysts; mechanism of reaction between TEAl dimer and NEt_3 to form NEt_3*TEAl adduct; WAXS patterns of PEs.

REFERENCES

(1) Baier, M. C.; Zuideveld, M. A.; Mecking, S. Post-Metallocenes in the Industrial Production of Polyolefins. *Angewandte Chemie International Edition International Edition*. 2014, pp 9722–9744. https://doi.org/10.1002/anie.201400799.

(2) Klosin, J.; Fontaine, P. P.; Figueroa, R. Development of Group IV Molecular Catalysts for High Temperature Ethylene-α-Olefin Copolymerization Reactions. *Acc. Chem. Res.* **2015**, *48* (7), 2004–2016. https://doi.org/10.1021/acs.accounts.5b00065.

(3) Stürzel, M.; Mihan, S.; Mülhaupt, R. From Multisite Polymerization Catalysis to Sustainable Materials and All-Polyolefin Composites. *Chem. Rev.* **2016**, *116* (3), 1398–1433. https://doi.org/10.1021/acs.chemrev.5b00310.

(4) Yuan, S. F.; Yan, Y.; Solan, G. A.; Ma, Y.; Sun, W. H. Recent Advancements in N-Ligated Group 4 Molecular Catalysts for the (Co)Polymerization of Ethylene. *Coordination Chemistry Reviews*. Elsevier B.V. 2020, p 213254.

https://doi.org/10.1016/j.ccr.2020.213254.

(5) Tan, C.; Chen, C. Emerging Palladium and Nickel Catalysts for Copolymerization of Olefins with Polar Monomers. *Angew. Chemie Int. Ed.* **2019**, *58* (22), 7192–7200. https://doi.org/10.1002/anie.201814634.

(6) Zanchin, G.; Bertini, F.; Vendier, L.; Ricci, G.; Lorber, C.; Leone, G. Copolymerization of Ethylene with Propylene and Higher α-Olefins Catalyzed by (Imido)Vanadium(Iv) Dichloride Complexes. *Polym. Chem.* **2019**, *10* (45). https://doi.org/10.1039/c9py01415b.

(7) Mahmood, Q.; Sun, W. H. N,N-Chelated Nickel Catalysts for Highly Branched Polyolefin Elastomers: A Survey. *R. Soc. Open Sci.* **2018**, *5* (7). https://doi.org/10.1098/rsos.180367.

(8) Xing, Y.; Wang, L.; Yu, H.; Khan, A.; Haq, F.; Zhu, L. Recent Progress in Preparation of Branched Polyethylene with Nickel, Titanium, Vanadium and Chromium Catalytic Systems and EPR Study of Related Catalytic Systems. *Eur. Polym. J.* **2019**, No. October, 109339. https://doi.org/10.1016/j.eurpolymj.2019.109339.

(9) Bariashir, C.; Huang, C.; Solan, G. A.; Sun, W. H. Recent Advances in Homogeneous Chromium Catalyst Design for Ethylene Tri-, Tetra-, Oligo- and Polymerization. *Coord. Chem. Rev.* **2019**, *385*, 208–229. https://doi.org/10.1016/j.ccr.2019.01.019.

(10) Liu, L.; Liu, Z.; Tang, S.; Cheng, R.; He, X.; Liu, B. What Triggered the Switching from Ethylene-Selective Trimerization into Tetramerization over the Cr/(2,2′-Dipicolylamine) Catalysts? *ACS Catal.* **2019**, *9* (11), 10519–10527. https://doi.org/10.1021/acscatal.9b03340.

(11) Martino, G. A.; Piovano, A.; Barzan, C.; Rabeah, J.; Agostini, G.; Bruekner, A.; Leone, G.; Zanchin, G.; Monoi, T.; Groppo, E. Rationalizing the Effect of Triethylaluminum on the Cr/SiO<inf>2</Inf> Phillips Catalysts. *ACS Catal.* **2020**, *10* (4). https://doi.org/10.1021/acscatal.9b04726.

(12) Jongkind, M. K.; van Kessel, T.; Velthoen, M. E. Z.; Friederichs, N.; Weckhuysen, B. M. Tuning the Redox Chemistry of a Cr/SiO2 Phillips Catalyst for Controlling Activity, Induction Period and Polymer Properties. *ChemPhysChem* **2020**, *21* (15), 1665–1674. https://doi.org/10.1002/cphc.202000488.

(13) McDaniel, M. Manipulating Polymerization Chemistry of Cr/Silica Catalysts through Calcination. *Appl. Catal. A Gen.* **2017**, *542*, 392–410.

https://doi.org/10.1016/j.apcata.2016.12.001.

(14) Mark, S.; Wadepohl, H.; Enders, M. Molecular Weight Control in Organochromium Olefin Polymerization Catalysis by Hemilabile Ligand-Metal Interactions. *Beilstein J. Org. Chem.* **2016**, *12*, 1372–1379. https://doi.org/10.3762/bjoc.12.131.

(15) Döhring, A.; Jensen, V. R.; Jolly, P. W.; Thiel, W.; Weber, J. C. Donor-Ligand-Substituted Cyclopentadienylchromium(III) Complexes: A New Class of Alkene Polymerization Catalyst. 2. Phosphinoalkyl-Substituted Systems. *Organometallics* **2001**, *20* (11), 2234–2245. https://doi.org/10.1021/om010146m.

(16) Alferov, K. A.; Belov, G. P.; Meng, Y. Chromium Catalysts for Selective Ethylene Oligomerization to 1-Hexene and 1-Octene: Recent Results. *Applied Catalysis A: General*. Elsevier B.V. July 25, 2017, pp 71–124. https://doi.org/10.1016/j.apcata.2017.05.014.

(17) Agapie, T. Selective Ethylene Oligomerization: Recent Advances in Chromium Catalysis and Mechanistic Investigations. *Coord. Chem. Rev.* **2011**, *255* (7–8), 861–880. https://doi.org/10.1016/j.ccr.2010.11.035.

(18) Huang, Y. B.; Jin, G. X. Half-Sandwich Chromium(III) Complexes Bearing β-Ketoiminato and β-Diketiminate Ligands as Catalysts for Ethylene Polymerization. *Dalt. Trans.* **2009**, *705206* (5), 767–769. https://doi.org/10.1039/b820798b.

(19) Xu, T.; Mu, Y.; Gao, W.; Ni, J.; Ye, L.; Tao, Y. Highly Active Half-Metallocene Chromium(III) Catalysts for Ethylene Polymerization Activated by Trialkylaluminum. *J. Am. Chem. Soc.* **2007**, *129* (8), 2236–2237. https://doi.org/10.1021/ja0671363.

(20) Gibson, V. C.; Mastroianni, S.; Newton, C.; Redshaw, C.; Solan, G. A.; White, A. J. P.; Williams, D. J. A Five-Coordinate Chromium Alkyl Complex Stabilised by Salicylaldiminato Ligands. *J. Chem. Soc. Dalt. Trans.* **2000**, *3* (13), 1969–1971. https://doi.org/10.1039/b002631j.

(21) Romano, D.; Ronca, S.; Rastogi, S. A Hemi-Metallocene Chromium Catalyst with Trimethylaluminum-Free Methylaluminoxane for the Synthesis of Disentangled Ultra-High Molecular Weight Polyethylene. *Macromol. Rapid Commun.* **2015**, *36* (3), 327–331. https://doi.org/10.1002/marc.201400514.

(22) Mark, S.; Kurek, A.; Mülhaupt, R.; Xu, R.; Klatt, G.; Köppel, H.; Enders, M. Hydridoboranes as Modifiers for Single-Site Organochromium Catalysts: From Low- to Ultrahigh-Molecular-Weight Polyethylene. *Angew. Chemie - Int. Ed.* **2010**, *49* (46),

8751–8754. https://doi.org/10.1002/anie.201003918.

(23) Despagnet-Ayoub, E.; Takase, M. K.; Henling, L. M.; Labinger, J. A.; Bercaw, J. E. Mechanistic Insights on the Controlled Switch from Oligomerization to Polymerization of 1-Hexene Catalyzed by an NHC-Zirconium Complex. *Organometallics* **2015**, *34* (19), 4707–4716. https://doi.org/10.1021/acs.organomet.5b00472.

(24) Belelli, P. G.; Ferreira, M. L.; Damiani, D. E. Addition of Lewis Bases and Acids. Effect on α-Olefins Polymerization with Soluble Metallocenes, 1. Ethylene. *Macromol. Chem. Phys.* **2000**, *201* (13), 1466–1475. https://doi.org/10.1002/1521-3935(20000801)201:13<1466::AID-MACP1466>3.0.CO;2-B.

(25) Belelli, P. G.; Ferreira, M. L.; Damiani, D. E. Addition of Lewis Bases and Acids. Effect on α-Olefins Polymerization with Soluble Metallocenes, 2. Propylene. *Macromol. Chem. Phys.* **2000**, *201* (13), 1466–1475. https://doi.org/10.1002/1521-3935(20000801)201:13<1466::AID-MACP1466>3.0.CO;2-B.

(26) Liu, H.; Wang, F.; Liu, L.; Dong, B.; Zhang, H. X.; Bai, C. X.; Hu, Y. M.; Zhang, X. Q. Synthesis, Characterization and 1,3-Butadiene Polymerization Behaviors of Three ONO, ONN, and NNN Tridentate Co(II) Complexes. *Inorganica Chim. Acta* **2014**, *421*, 284–291. https://doi.org/10.1016/j.ica.2014.06.010.

(27) Cariou, R.; Chirinos, J. J.; Gibson, V. C.; Jacobsen, G.; Tomov, A. K.; Britovsek, G. J. P.; White, A. J. P. The Effect of the Central Donor in Bis(Benzimidazole)-Based Cobalt Catalysts for the Selective Cis-1,4-Polymerisation of Butadiene. *Dalt. Trans.* **2010**, *39* (38), 9039–9045. https://doi.org/10.1039/c0dt00402b.

(28) Lang, J. R. V.; Denner, C. E.; Alt, H. G. Homogeneous Catalytic Dimerization of Propylene with Bis(Imino)Pyridine Vanadium(III) Complexes. *J. Mol. Catal. A Chem.* **2010**, *322* (1–2), 45–49. https://doi.org/10.1016/j.molcata.2010.02.013.

(29) Messinis, A. M.; Messinis, A. M.; Wright, W. R. H.; Wright, W. R. H.; Hanton, M. J.; Dyer, P. W.; Dyer, P. W. Additives Boosting the Performance of Tungsten Imido-Mediated Ethylene Dimerization Systems for Industrial Application. *Chem. Commun.* **2020**, *56* (50), 6886–6889. https://doi.org/10.1039/d0cc03077e.

(30) Wang, G.; Li, M.; Pang, W.; Chen, M.; Tan, C. Lewis Acids: In Situ Modulate Pyridazine-Imine Ni Catalysed Ethylene (Co)Polymerisation. *New J. Chem.* **2019**, *43* (34), 13630–13634. https://doi.org/10.1039/c9nj01243e.

(31) Zubkevich, S. V.; Tuskaev, V. A.; Gagieva, S. C.; Pavlov, A. A.; Khrustalev, V. N.; Polyakova, O. V.; Zarubin, D. N.; Kurmaev, D. A.; Kolosov, N. A.; Bulychev, B. M. Catalytic Systems Based on Nickel(Ii) Complexes with Bis(3,5-Dimethylpyrazol-1-Yl)Methane-Impact of PPh3 on the Formation of Precatalysts and Selective Dimerization of Ethylene. *New J. Chem.* **2020**, *44* (3), 981–993. https://doi.org/10.1039/c9nj05704h.

(32) Tan, C.; Qasim, M.; Pang, W.; Chen, C. Ligand-Metal Secondary Interactions in Phosphine-Sulfonate Palladium and Nickel Catalyzed Ethylene (Co)Polymerization. *Polym. Chem.* **2020**, *11* (2), 411–416. https://doi.org/10.1039/c9py00904c.

(33) Leone, G.; Groppo, E.; Zanchin, G.; Martino, G. A.; Piovano, A.; Bertini, F.; Martí-Rujas, J.; Parisini, E.; Ricci, G. Concerted Electron Transfer in Iminopyridine Chromium Complexes: Ligand Effects on the Polymerization of Various (Di)Olefins. *Organometallics* **2018**, *37* (24). https://doi.org/10.1021/acs.organomet.8b00812.

(34) McGuinness, D. S. Olefin Oligomerization via Metallacycles: Dimerization, Trimerization, Tetramerization, and Beyond. *Chemical Reviews*. American Chemical Society March 9, 2011, pp 2321–2341. https://doi.org/10.1021/cr100217q.

(35) Zaccaria, F.; Sian, L.; Zuccaccia, C.; Macchioni, A. *Ion Pairing in Transition Metal Catalyzed Olefin Polymerization*, 1st ed.; Elsevier Inc., 2020; Vol. 73. https://doi.org/10.1016/bs.adomc.2019.08.001.

(36) Eilertsen, J. L.; Støvneng, J. A.; Ystenes, M.; Rytter, E. Activation of Metallocenes for Olefin Polymerization as Monitored by IR Spectroscopy. *Inorg. Chem.* **2005**, *44* (13), 4843–4851. https://doi.org/10.1021/ic0482638.

(37) Chen, E. Y. X.; Marks, T. J. Cocatalysts for Metal-Catalyzed Olefin Polymerization: Activators, Activation Processes, and Structure-Activity Relationships. *Chem. Rev.* **2000**, *100* (4), 1391–1434. https://doi.org/10.1021/cr980462j.

(38) Nomura, K.; Zhang, S. Design of Vanadium Complex Catalysts for Precise Olefin Polymerization. *Chem. Rev.* **2011**, *111* (3), 2342–2362. https://doi.org/10.1021/cr100207h.

(39) Makio, H.; Prasad, A. V.; Terao, H.; Saito, J.; Fujita, T. Isospecific Propylene Polymerization with in Situ Generated Bis(Phenoxy-Amine)Zirconium and Hafnium Single Site Catalysts. *Dalt. Trans.* **2013**, *42* (25), 9112–9119. https://doi.org/10.1039/c3dt00058c.

(40) Matsui, S.; Mitani, M.; Saito, J.; Tohi, Y.; Makio, H.; Matsukawa, N.; Takagi, Y.; Tsuru, K.; Nitabaru, M.; Nakano, T.; Tanaka, H.; Kashiwa, N.; Fujita, T. A Family of Zirconium Complexes Having Two Phenoxy - Imine Chelate Ligands for Olefin Polymerization. *J. Am. Chem. Soc.* **2001**, *123* (28), 6847–6856. https://doi.org/10.1021/ja0032780.

(41) Tritto, I.; Sacchi, M. C.; Locatelli, P.; Li, S. X. Metallocene Ion Pairs: A Direct Insight into the Reaction Equilibria and Polymerization by ^{13}C NMR Spectroscopy. *Macromol. Symp.* **1995**, *89* (1), 289–298. https://doi.org/10.1002/masy.19950890128.

(42) Tritto, I.; Sacchi, M. C.; Li, S. NMR Study of the Reactions in Cp2TiMeCl/AlMe3 and Cp2TiMeCl/Methylalumoxane Systems, Catalysts for Olefin Polymerization. *Macromol. Rapid Commun.* **1994**, *15* (3), 217–223. https://doi.org/10.1002/marc.1994.030150306.

(43) Talebi, S.; Duchateau, R.; Rastogi, S.; Kaschta, J.; Peters, G. W. M.; Lemstra, P. J. Molar Mass and Molecular Weight Distribution Determination of UHMWPE Synthesized Using a Living Homogeneous Catalyst. *Macromolecules* **2010**, *43* (6), 2780–2788. https://doi.org/10.1021/ma902297b.

(44) Zijlstra, H. S.; Joshi, A.; Linnolahti, M.; Collins, S.; McIndoe, J. S. Interaction of Neutral Donors with Methylaluminoxane. *Eur. J. Inorg. Chem.* **2019**, *2019* (18), 2346–2355. https://doi.org/10.1002/ejic.201900153.

(45) Fatou, J. G.; Mandelkern, L. The Effect of Molecular Weight on the Melting Temperature and Fusion of Polyethylene. *J. Phys. Chem.* **1965**, *69*, 417–428. https://doi.org/10.1021/j100886a010.

(46) Zhang, W.; Sun, W. H.; Zhang, S.; Hou, J.; Wedeking, K.; Schultz, S.; Fröhlich, R.; Song, H. Synthesis, Characterization, and Ethylene Oligomerization and Polymerization of [2,6-Bis(2-Benzimidazolyl)Pyridyl]Chromium Chlorides. *Organometallics* **2006**, *25* (8), 1961–1969. https://doi.org/10.1021/om050805l.

(47) Chien, J. C. W.; He, D. Olefin Copolymerization with Metallocene Catalysts. II. Kinetics, Cocatalyst, and Additives. *J. Polym. Sci. Part A Polym. Chem.* **1991**, *29* (11), 1595–1601. https://doi.org/10.1002/pola.1991.080291108.

(48) Kvisle, S.; Rytter, E. Infrared Matrix Isolation Spectroscopy of Trimethylgallium, Trimethylaluminium and Triethylaluminium. *Spectrochim. Acta Part A Mol. Spectrosc.* **1984**, *40* (10), 939–951. https://doi.org/10.1016/0584-8539(84)80153-1.

(49) Imhoff, D. W.; Simeral, L. S.; Sangokoya, S. A.; Peel, J. H. Characterization of Methylaluminoxanes and Determination of Trimethylaluminum Using Proton NMR. *Organometallics* **1998**, *17* (10), 1941–1945. https://doi.org/10.1021/om980046p.

(50) Barron, A. R. New Method for the Determination of the Trialkylaluminum Content in Alumoxanes. *Organometallics* **1995**, *14* (7), 3581–3583. https://doi.org/10.1021/om00007a070.

(51) Odom, J. D.; Barnes, J. A.; Hudgens, B. A.; Durig, J. R. Spectra and Structure of Boron-Nitrogen Compounds. II. Infrared and Raman Spectra of Trimethylamine-Borane. *J. Phys. Chem.* **1974**, *78* (15), 1503–1509. https://doi.org/10.1021/j100608a012.

(52) Barron, A. R. Adducts of Trimethylaluminium with Phosphine Ligands; Electronic and Steric Effects. *J. Chem. Soc. Dalt. Trans.* **1988**, No. 12, 3047–3050. https://doi.org/10.1039/DT9880003047.

(53) Busico, V.; Cipullo, R.; Cutillo, F.; Friederichs, N.; Ronca, S.; Wangt, B. Improving the Performance of Methylalumoxane: A Facile and Efficient Method to Trap "Free" Trimethylaluminum. *J. Am. Chem. Soc.* **2003**, *125* (41), 12402–12403. https://doi.org/10.1021/ja0372412.

(54) Ehm, C.; Cipullo, R.; Budzelaar, P. H. M.; Busico, V. Role(s) of TMA in Polymerization. *Dalt. Trans.* **2016**, *45*, 6847. https://doi.org/10.1039/c5dt04895h.

(55) Zaccaria, F.; Budzelaar, P. H. M.; Cipullo, R.; Zuccaccia, C.; Macchioni, A.; Busico, V.; Ehm, C. Reactivity Trends of Lewis Acidic Sites in Methylaluminoxane and Some of Its Modifications. *Inorg. Chem.* **2020**, *59* (8), 5751–5759. https://doi.org/10.1021/acs.inorgchem.0c00533.

(56) Macchioni, A. Ion Pairing in Transition-Metal Organometallic Chemistry. *Chemical Reviews*. American Chemical Society June 2005, pp 2039–2073. https://doi.org/10.1021/cr0300439.

FOR TABLE OF CONTENTS ONLY